Theory of energy transfer interactions near sphere and nanoshell based plasmonic nanostructures

Manmohan S. Shishodia,[*,1,2] Boris D. Fainberg,[1,2] and Abraham Nitzan[1]
[1]School of Chemistry, Tel Aviv University, Tel Aviv 69978, Israel
[2]Faculty of Sciences, Holon Institute of Technology, 52 Golomb St., Holon 58102, Israel

Abstract
Theory of energy transfer interactions between a pair of two level molecules in the molecular nanojunction including surface plasmon (SP) dressed interaction of plasmonic nanostructure, replicating metallic leads is presented. Results on the modification of bare dipolar interaction, known to be responsible for molecular energy transfer processes, in the proximity of metallic nanosystem are presented. Specifically, the manuscript includes theoretical investigation of nanosphere (NSP) monomer, nanoshell (NSH) monomer, and coupled nanosphere pair (dimer) based nanosystems. Closed form analytical expressions for NSP and NSH structures tailored for molecular nanojunction geometry are derived in the theoretical framework of multipole spectral expansion (MSE) method, which is straightforwardly extendible to dimers and multimers. The role of size and dielectric environment on energy transfer is investigated and interpreted. Theory predicts that the monomer and dimer both enhance the dipolar interaction, yet, dimer geometry is favorable due to its spectral tuning potential originated from plasmon hybridization and true resemblance with typical molecular nanojunctions.

Keywords: Plasmonic nanostructure, surface plasmon, nanoshell, energy transfer, exciton, dipole, molecular nanojunction, nanoparticle dimer.

1. Introduction

Metallic nanostructures (MNSs) have found immense real life applications in e.g., molecular spectroscopy, sensing, detection, medical diagnostics, optoelectronic integration etc., to name only a few. Extensive applications and multitude of fascinating nano-regime phenomena linked to MNSs primarily originate from their ability to enhance and concentrate electromagnetic field (EMF) by virtue of surface plasmon (SP) excitation, the quanta of collective free electron oscillations [1]. Continuum of already known applications in conjunction with the scope of tremendous unexplored potential has given an ever increasing impetus to the theoretical as well as experimental investigation of variety of MNSs, including but not limited to spherical, spheroidal, cubic, rods, star, and triangular prisms [2]. Isolated spherical metallic nanoparticle and coupled metallic nanoparticle pair (dimer) has attracted a great deal of attention to investigate various phenomena occurring in the world of plasmonics. In addition to the nanoparticle monomer, coupled nanoparticles have also been widely investigated and proved to be useful in e.g., surface enhanced Raman scattering (SERS), nano-scale optical wave-guiding, detection, nanolensing, phase tuning of the nonlinear susceptibility, enhancement of molecular fluorescence, and quantum-dots (QDs) photoluminescence [3-6]. Coupled nanoparticle dimers have widely been investigated using hybridization theory where

* Corresponding author E-Mail: manmohaniitd@gmail.com

Plasmonics: Metallic Nanostructures and Their Optical Properties IX, edited by Mark I. Stockman,
Proc. of SPIE Vol. 8096, 80961G · © 2011 SPIE · CCC code: 0277-786X/11/$18 · doi: 10.1117/12.892940

SP modes of a complex nanostructure are expressed as the bonding (symmetric) and the antibonding (asymmetric) interaction of SPs belonging to the constituents [7, 8]. Another class of MNS similar to NSP but exhibiting rich plasmonic features is nanoshell (NSH) [9, 10], which provide scope for spectral fine-tuning of SP frequencies in its monomer geometry itself. This is possible by virtue of controlling sphere and cavity plasmon interaction through core/shell dimensions. In addition, NSHs are expected to: (I) show greater sensitivity to the change of dielectric environment, (II) allow controllable redirection of electromagnetic radiation, (III) facilitate study of multipole surface plasmon resonances (SPRs). Although numerous studies have been undertaken concerning monomer and dimer of solid as well as shell based MNSs, but for the most part, studies focus on the MNSs excited by uniform electric field or plane waves. In the recent years, the study of molecular exciton-metallic nanostructure complexes has attracted attention of researchers and the efforts investigating plasmonic-excitonic (plexcitonic) interactions have gained unprecedented impetus; see, e.g., [11, 12] and references cited therein. Still the issue concerning modification of dipolar interaction between molecules located in the proximity of MNSs or in the junction region and its implications on molecular junction/bridge characteristics has not found due attention. It is expected that the excitonic (energy transfer) interactions accompanied by plasmonic response of metallic contacts/leads can have substantial effect on the electronic transport properties of molecular nanojunction [13]. Here, we address this issue and extend well known Gersten-Nitzan theory [14, 15] for spheroidal particle to examine the issue concerning molecular wire and junction. In view of the close resemblance of pair of metallic particles (dimer) and real molecular nanojunction system, we shall consider NSP dimer in addition to NSP and NSH monomers. Due to the plasmonic hybridization, dimer nanostructures may induce a relatively intense local EMF within the dimer gap region and in the proximity of MNS. We shall show that the dimer spectrum can be fine tuned to achieve the enhancement in the desired spectral window through engineering of the dimer parameters. For the proposed geometry to be studied here, specific multipoles can be made to dominate through proper choice of system parameters e.g., size, shape, and dipole-dipole separation. These observations are in sharp contrast to the situation where two molecules are located at diametrically opposite ends of the nanoparticle [10, 14]. Instead of direct solution approach used in [14, 15], we shall adopt multipole spectral expansion (MSE) based approach for the present study, since MSE based formalism separates the geometrical and dielectric properties and can be extended to the arbitrary combination of nanoparticles. It may be anticipated that SP enhanced EMF can greatly alter the molecular interactions in the excitonic and energy transfer donor-acceptor system. Plexcitonic coupling in this case will strongly affect the current conduction in the molecular wire. Moreover, plexcitonic coupling can have applications e.g., in the: (I) study of energy transfer through a plasmonic structure between the quantum dots (QDs), (II) light up-conversion, (III) carrier density enhancement near molecular system or the material, (IV) enhancement of cross-section of chemical reactions. In this manuscript, we present a unified approach based on multipole spectral expansion (MSE) method for a systematic study of molecular energy transfer interactions in the proximity of NSP monomer, NSH monomer, and NSP dimer (coupled NSPs). We shall show that the energy transfer in a molecular wire between two metallic contacts representing a nanoparticle dimer is enhanced and the spectrum can be fine tuned through controlling dimer parameters.

The manuscript is organized as follows. Section 2 describes the theoretical formulation of the problem and its implementation to the monomer of NSP and NSH and the dimer of NSP. Sec. 3 discusses the results of our investigation. Finally, Sec. 4 presents an overall summary, concluding remarks and future direction of the work.

2. Theoretical Model

2.1 Formulation of the Problem

Schematics of the plexcitonic system subjected to the present study are shown in Fig.1. Terminology and symbols adopted in this manuscript are explained in the figure captions. We shall adopt multipole spectral expansion (MSE) method originally introduced by Fuchs [16] to investigate the optical properties of ionic crystals and further developed by Bergman [17, 18], Milton [19], and Stockman et *al*. [20], to investigate the energy transfer between a pair of molecules (for definiteness we label one of them as a donor and another one as an acceptor) located in the proximity of a metallic nanosystem. Unless mentioned otherwise, both molecules represented by their transition dipole moments ($\mathbf{p}_d$ and $\mathbf{p}_a$) will be assumed to be located on the $+z$ axis (outside metallic region) and oriented along $\hat{\mathbf{z}}$ direction. We shall see that the monomer can be analyzed through closed form

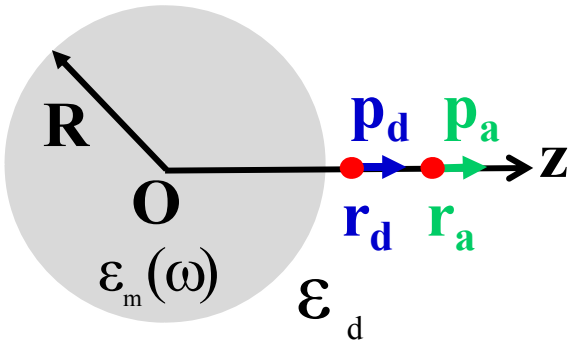

Fig. 1(a): Schematic picture showing a pair of two level molecular system (labeled acceptor-a, and donor-d for definiteness) in the proximity of NSP monomer of radius R. The molecules are represented by their dipole moments $\mathbf{p}_d$ and $\mathbf{p}_a$, located at $\mathbf{r}_d$ and $\mathbf{r}_a$, and oriented along $\hat{\mathbf{z}}$ direction.

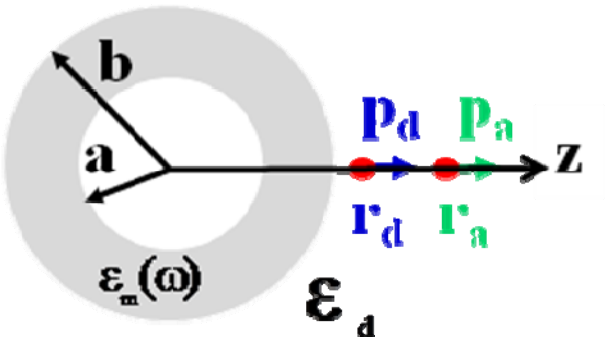

Fig. 1(b): Schematic picture showing a pair of two level molecular system (labeled acceptor-a, and donor-d for definiteness) in the proximity of NSH monomer of inner and outer radii, a and b, respectively. Other parameters are the same as in Fig. 1(a).

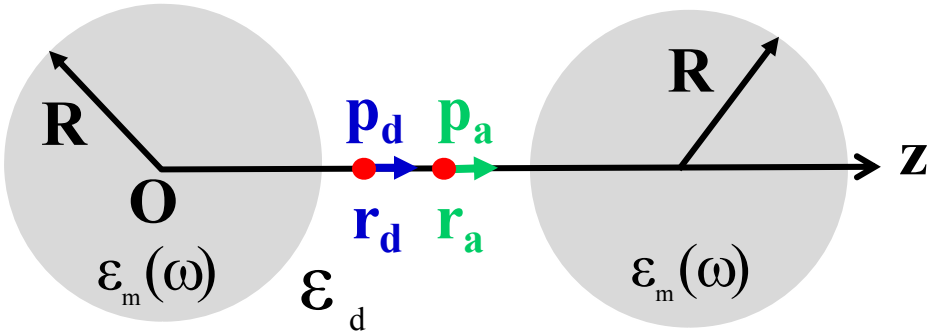

Fig. 1(c): Schematic picture showing a pair of two level molecular system (labeled as acceptor-a and donor-d for definiteness) in the junction region of NSP dimer consisting of identical spheres of radii R. The molecules are represented by their dipole moments $\mathbf{p}_d$ and $\mathbf{p}_a$, located at $\mathbf{r}_d$ and $\mathbf{r}_a$ (relative to O), and oriented parallel to the symmetry axis. This geometry more closely mimics a typical molecular nanojunction, where plasmon hybridization [7, 8] may generate strong electromagnetic enhancement.

analytical expressions, and dimer through interaction matrix based approach. Metallic nanosystem may be described through frequency (ω) dependent dielectric function, $\varepsilon_m(\omega)$ and assumed to be embedded in a host medium characterized by its dielectric permittivity, ε_d. Local response of the whole system is described by a space and frequency dependent dielectric function, $\varepsilon(\mathbf{r},\omega)$ defined as,

$$\varepsilon(\mathbf{r},\omega) = \varepsilon_m(\omega)\Theta(\mathbf{r}) + \varepsilon_d[1-\Theta(\mathbf{r})] \tag{1}$$

where, $\Theta(\mathbf{r})$ is the characteristic function of the system under consideration with value 1 in the metal and 0 in the embedded medium, hence digitally dividing active and passive regions of the system. Limiting our analysis to the total system size much less than the wavelength of light equivalent to the molecular transition frequency (ω), where quasistatic approach is valid, the electrostatic potential $\varphi(\mathbf{r})$ must satisfy,

$$\nabla \bullet \left[\varepsilon(\mathbf{r},\omega)\nabla\varphi(\mathbf{r})\right] = 0 \tag{2}$$

Substitution of local response function $\varepsilon(\mathbf{r},\omega)$ from Eq.1 into Eq.2 produces,

$$\nabla \bullet \left\{\varepsilon_m(\omega)\Theta(\mathbf{r}) + \varepsilon_d[1-\Theta(\mathbf{r})]\right\}\nabla\varphi(\mathbf{r}) = 0 \tag{3}$$

or,

$$\nabla^2\varphi(\mathbf{r}) = \left[1 - \left\{\varepsilon_m(\omega)/\varepsilon_d\right\}\right]\left[\nabla \bullet \Theta(\mathbf{r})\nabla\varphi(\mathbf{r})\right] \tag{4}$$

Let us now introduce spectral parameters, $u(\omega)$ and $s(\omega)$ defined as,

$$s(\omega) = \left[1 - \left\{\varepsilon_m(\omega)/\varepsilon_d\right\}\right]^{-1},\ u(\omega) = 1/s(\omega) \tag{5}$$

Then Eq. 4 can be written in the form of spectral parameters as,

$$\nabla^2\varphi(\mathbf{r}) = u(\omega)\left[\nabla \bullet \left\{\Theta(\mathbf{r})\nabla\varphi(\mathbf{r})\right\}\right]$$

or

$$\nabla \bullet \left[\Theta(\mathbf{r})\nabla\varphi(\mathbf{r})\right] = s(\omega)\nabla^2\varphi(\mathbf{r}) \tag{6}$$

The corresponding eigenvalue problem is,

$$\nabla \bullet [\Theta(\mathbf{r})\ \nabla\psi_\lambda(\mathbf{r})] = s_\lambda\nabla^2\psi_\lambda(\mathbf{r}) \tag{7}$$

Eq. 7 has solutions $\{\psi_\lambda(\mathbf{r})\}$ corresponding to the values, $s(\omega) = s_\lambda$. Therefore, we will have to solve Eq. 6 (equivalently, Eq. 7) for the system under investigation. The formal solution to the Eq. 6 with $\varphi_{ext}(\mathbf{r})$ as the external electric potential may be written in terms of vacuum Green's function G_0 as [17, 18],

$$\varphi(\mathbf{r}) = \varphi_{ext}(\mathbf{r}) - u(\omega)\iiint d^3r' G_0(\mathbf{r},\mathbf{r}')\nabla' \bullet \left[\Theta(\mathbf{r}')\nabla'\varphi(\mathbf{r}')\right] \tag{8}$$

$$= \varphi_{ext}(\mathbf{r}) + u(\omega)\Gamma\varphi(\mathbf{r}) \tag{9}$$

where, Γ is defined as,

$$\Gamma\varphi(\mathbf{r}) = \iiint d^3r'\Theta(\mathbf{r}')[\nabla' G_0(\mathbf{r},\mathbf{r}')]\nabla'\varphi(\mathbf{r}') \tag{10}$$

Let us defining a scalar product of two eigenfunctions as,

$$\left\langle \psi_\lambda(\mathbf{r}) \,|\, \psi_{\lambda'}(\mathbf{r}) \right\rangle = \iiint_V \Theta(\mathbf{r})\nabla\psi_\lambda^*(\mathbf{r})\nabla\psi_{\lambda'}(\mathbf{r})\,d^3r = \delta_{\lambda,\lambda'} \tag{11}$$

We would like to emphasize that the scalar product in Eq.11 is defined inside the metallic region only. $\psi_\lambda^*(\mathbf{r})$ denotes the complex conjugated and δ is the Kronecker delta symbol. In case of zero external potential, Eq. 9 can be written as,

$$s(\omega)\varphi(\mathbf{r}) = \Gamma\varphi(\mathbf{r}) \tag{12}$$

Eq. 12 corresponds to the homogeneous counterpart of the full equation and may be written in the eigenvalue form as,

$$s_{\lambda}\psi_{\lambda}(\mathbf{r}) = \Gamma\,\psi_{\lambda}(\mathbf{r}) \tag{13}$$

Since Eq. 13 is the solution of Eq. 7, eigenfunctions and eigenvalues of operator Γ are the same as solutions of Eq. 6. Eigencharacteristics (eigenvalues and eigenfunctions) for single inclusion (here nanosphere) can be determined analytically by imposing the boundary and the orthonormalization conditions. To determine them uniquely, we seek these eigenfunctions in the form of spherical harmonics as,

$$\psi^{\text{in}}_{lm}(\mathbf{r}) = \mathrm{A}_{lm}\,\mathrm{r}^{l}\mathrm{Y}_{lm}(\theta,\phi), \qquad \text{for } \mathrm{r} < \mathrm{R} \tag{14}$$

$$\psi^{\text{out}}_{lm}(\mathbf{r}) = \mathrm{B}_{lm}\,\frac{\mathrm{Y}_{lm}(\theta,\phi)}{\mathrm{r}^{l+1}}, \qquad \text{for } \mathrm{r} > \mathrm{R} \tag{15}$$

where $\mathbf{r} = (\mathrm{r},\theta,\phi)$ denotes spherical coordinates relative to the origin at the centre of nanosphere (see, Fig. 1.a). Superscript, in (out) refers to the region inside (outside) NSP. The system boundaries are assumed to be placed infinitely away from the spherical inclusion. It may be noticed that the homogeneous differential equation is automatically satisfied by these functions except at the surface of the sphere where we will have to impose additional electrostatic boundary conditions stated as,

$$\text{(i)}\ \ \psi^{\text{in}}_{lm}(\mathbf{r})\big|_{\mathrm{r=R}} = \psi^{\text{out}}_{lm}(\mathbf{r})\big|_{\mathrm{r=R}} \tag{16}$$

$$\text{(ii)}\ \ \varepsilon_{\mathrm{m}}(\omega)\frac{\partial\psi^{\text{in}}_{lm}(\mathbf{r})}{\partial\,\mathrm{r}}\bigg|_{\mathrm{r=R}} = \varepsilon_{\mathrm{d}}\,\frac{\psi^{\text{out}}_{lm}(\mathbf{r})}{\partial\,\mathrm{r}}\bigg|_{\mathrm{r=R}} \tag{17}$$

Application of these boundary conditions produces,

$$\mathrm{B}_{lm} = \mathrm{A}_{lm}\,\mathrm{R}^{2l+1} \tag{18}$$

$$\varepsilon_{\mathrm{m}}(\omega) = -\frac{(l+1)}{l}\varepsilon_{\mathrm{d}} \tag{19}$$

Therefore,

$$\mathrm{s}(\omega) = \frac{1}{\left[1-\{\varepsilon_{\mathrm{m}}(\omega)/\varepsilon_{\mathrm{d}}\}\right]} = \frac{l}{2l+1} \tag{20}$$

Let us now determine the coefficients uniquely by imposing the orthonormalization condition, (Eq. 11). The evaluation can be greatly simplified by using the following Green's identity [21, 22],

$$\iiint_{\mathrm{V}}\left(\varphi\nabla^2\psi + \nabla\varphi.\nabla\psi\right)\mathrm{d}^3\mathrm{x} = \oiint_{\mathrm{S}}\varphi\frac{\partial\psi}{\partial\mathrm{n}}\mathrm{dA} \tag{21}$$

where $\frac{\partial\psi}{\partial\mathrm{n}}\mathrm{dA} = \nabla\psi.\hat{\mathbf{n}}$, and $\frac{\partial}{\partial\,\mathrm{n}}$ is the normal derivative at the surface S (directed outward from inside). Eq. 11 therefore can be written as,

$$\left\langle\psi_{lm}(\mathbf{r})\,|\,\psi_{l'm'}(\mathbf{r})\right\rangle = \oiint_{\mathrm{S}}\psi^{*}_{l\mathrm{m}}\frac{\partial\psi_{l'm'}}{\partial\,\mathrm{r}}\mathrm{r}^2\mathrm{d}\Omega - \iiint_{\mathrm{V}}\Theta(\mathbf{r})\left[\psi^{*}_{l\mathrm{m}}\nabla^2\psi_{l'm'}\right]\mathrm{d}^3\mathrm{r} \tag{22}$$

Integral, $\iiint_{\mathrm{V}}\Theta(\mathbf{r})\left[\psi^{*}_{l\mathrm{m}}\nabla^2\psi_{l'm'}\right]\mathrm{d}^3\mathrm{r}$ in Eq. 22 will be zero since the electrostatic eigenstates obey Laplace equation,

$$\nabla^2\psi_{l'm'} = 0 \tag{23}$$

Hence, we are left with the surface integral only. Equation 22 therefore produces,

$$\left\langle \psi_{lm}(\mathbf{r}) \,|\, \psi_{l'm'}(\mathbf{r}) \right\rangle = \mathrm{A}_{lm}{}^{2} l\, \mathrm{R}^{2l+1} \delta_{ll'} \delta_{mm'} \tag{24}$$

Finally, we get,

$$\mathrm{A}_{lm} = \frac{1}{\sqrt{l\, \mathrm{R}^{2l+1}}}, \text{ and } \quad \mathrm{B}_{lm} = \sqrt{\frac{\mathrm{R}^{2l+1}}{l}} \tag{25}$$

We can now summarize the eigencharacteristics of the NSP monomer as,

$$s_l = \frac{l}{2l+1} \tag{26}$$

$$\psi_{lm}^{in}(\mathbf{r}) = \frac{1}{\sqrt{l\, \mathrm{R}^{2l+1}}} \mathrm{r}^{l}\, \mathrm{Y}_{l\mathrm{m}}(\theta, \phi), \qquad \text{for } \mathrm{r} < \mathrm{R} \tag{27}$$

$$\psi_{l\,\mathrm{m}}^{out}(\mathbf{r}) = \sqrt{\frac{\mathrm{R}^{2l+1}}{l}} \frac{\mathrm{Y}_{l\mathrm{m}}(\theta, \phi)}{\mathrm{r}^{l+1}}, \qquad \text{for } \mathrm{r} > \mathrm{R} \tag{28}$$

Once we know the eigenvalues and eigenstates of operator Γ, we can generalize the solutions for the external electric potential, say $\varphi_{\mathrm{ext}}(\mathbf{r})$. Using the completeness condition,

$$\mathrm{I} = \sum_{\lambda} \; |\psi_{\lambda}(\mathbf{r})\rangle \langle \psi_{\lambda}(\mathbf{r})| \tag{29}$$

we get from Eq. 9, indexing the eigenstates λ as l, m

$$\varphi(\mathbf{r}) = \varphi_{\mathrm{ext}}(\mathbf{r}) + \sum_{lm} \frac{\mathrm{s}_l}{\mathrm{s}(\omega) - \mathrm{s}_l} \left\langle \Theta(\mathbf{r}) \psi_{lm}(\mathbf{r}) \,|\, \varphi_{\mathrm{ext}}(\mathbf{r}) \right\rangle \psi_{lm}(\mathbf{r}) \tag{30}$$

Equation 30 is the general expression for calculating the electrostatic potential at point $\mathbf{r}$ of the system due to the external electric potential $\varphi_{\mathrm{ext}}(\mathbf{r})$. Notably, $\varphi_{\mathrm{ext}}(\mathbf{r})$ may be originated from various sources e.g., uniform field, plane wave, and assembly of charges.

2.2 Generalization to the Plexcitonic System

In order to tailor MSE based approach to the plexcitonic system, we will have to determine the spherical potential $\varphi_{\mathrm{ext}}(\mathbf{r})$ at the point $\mathbf{r} = (\mathrm{r}, \theta, \phi)$ due to the point dipole positioned at $\mathbf{r}_j = (\mathrm{r}_j, \theta_j, \phi_j)$, which can be expressed as [15],

$$\varphi_{\mathrm{ext}}(\mathbf{r}) = \sum_{l'm'} \Phi_{l'm',\mathrm{j}}(\mathbf{r}) \tag{31}$$

The index j label the molecule/dipole (donor or acceptor). If the dipole moment vector is denoted by $\mathbf{p}_j$, Eq. 31 may be written as [15],

$$\varphi_{\mathrm{ext}}(\mathbf{r}) = \mathbf{p}_j \bullet \nabla_j \frac{1}{|\mathbf{r} - \mathbf{r}_j|} \tag{32}$$

where, ∇_j and $\mathbf{p}_j$ are defined in the spherical polar coordinates as follows,

$$\nabla_j = \hat{e}_{\mathrm{r}} \frac{\partial}{\partial \mathrm{r}_j} + \hat{e}_{\theta} \frac{1}{\mathrm{r}_j} \frac{\partial}{\partial \theta_j} + \hat{e}_{\phi} \frac{1}{\mathrm{r}_j \sin\theta_j} \frac{\partial}{\partial \phi_j} \tag{33}$$

$$\mathbf{p}_j = \hat{e}_{\mathrm{r}}\, \mathrm{p}_{\mathrm{r}} + \hat{e}_{\theta}\, \mathrm{p}_{\theta} + \hat{e}_{\phi}\, \mathrm{p}_{\varphi} \tag{34}$$

Using the expansion of the Green's function term, Eq. 32 may be written as,

$$\varphi_{\text{ext}}(\mathbf{r}) = \mathbf{p}_j \bullet \nabla_j \left(4\pi \sum_{l'm'} \frac{1}{(2l'+1)} \frac{\mathrm{r}_<^{l'}}{\mathrm{r}_>^{l'+1}} \mathrm{Y}^*_{l'\mathrm{m}'}(\theta_j, \phi_j) \mathrm{Y}_{l'\mathrm{m}'}(\theta, \phi) \right) \tag{35}$$

where the symbols have their usual meanings. Considering molecular orientations to be parallel to the +z-axis, we can write [21],

$$\varphi_{\text{ext}}(\mathbf{r}) = 4\pi \mathrm{p}_\mathrm{r} \sum_{l'm'} \frac{1}{(2l'+1)} \frac{\partial}{\partial \mathrm{r}_j} \left(\frac{\mathrm{r}_<^{l'}}{\mathrm{r}_>^{l'+1}} \right) \mathrm{Y}^*_{l'\mathrm{m}'}(\theta_j, \phi_j) \mathrm{Y}_{l'\mathrm{m}'}(\theta, \phi) \tag{36}$$

For a dipole situated outside the inclusion, the valid expression after considering the effect of embedded medium is,

$$\varphi_{\text{ext}}(\mathbf{r}) = \frac{4\pi \mathrm{p}_\mathrm{r}}{\varepsilon_\mathrm{d}} \sum_{l'm'} \frac{-(l'+1)}{(2l'+1)} \left(\frac{\mathrm{r}^{l'}}{\mathrm{r}_j^{l'+2}} \right) \mathrm{Y}^*_{l'\mathrm{m}'}(\theta_j, \phi_j) \mathrm{Y}_{l'\mathrm{m}'}(\theta, \phi) \tag{37}$$

Since, we now know the external potential in the multipolar expansion form, the overlap integral (say, I_{lm}) of $\varphi_{\text{ext}}(\mathbf{r})$ and the NSP eigenmodes can be calculated as,

$$\mathrm{I}_{lm} = \left\langle \Theta(\mathbf{r}) \psi_{l\mathrm{m}} \mid \varphi_{\text{ext}}(\mathbf{r}) \right\rangle = \iiint_\mathrm{V} \Theta(\mathbf{r}) \, \mathrm{d}^3\mathrm{r} \left[\nabla \psi^*_{l\,\mathrm{m}} . \nabla \varphi_{\text{ext}}(\mathbf{r}) \right] \tag{38}$$

It should be noted that ψ_{lm} here refers to the inner eigenmodes of the nanosphere and $\varphi_{\text{ext}}(\mathbf{r})$ refers to the external excitation potential due to one of the molecule/dipole. Employing Green's identity (Eq. 21) and the Laplace equation (Eq. 23), Eq. 38 can be rewritten as,

$$\begin{aligned} \mathrm{I}_{lm} &= \oiint_{S,\mathrm{r}=\mathrm{R}} \varphi_{\text{ext}}(\mathbf{r}) \frac{\partial \psi^*_{l\mathrm{m}}}{\partial \mathrm{r}} \mathrm{dA} \\ &= -\frac{4\pi \mathrm{p}_j}{\varepsilon_\mathrm{d}} \sqrt{\frac{l}{\mathrm{R}^3}} \frac{(l+1)}{(2l+1)} \left(\frac{\mathrm{R}}{\mathrm{r}_\mathrm{j}} \right)^{l+2} \mathrm{Y}^*_{l\mathrm{m}}(\theta_j, \phi_j) \end{aligned} \tag{39}$$

Now bearing in mind that $\mathrm{Y}^*_{l\mathrm{m}}(\theta_j, \phi_j) = \mathrm{Y}^*_{l0}(0,0) = \sqrt{(2l+1)/4\pi}$, the electric potential can be written as,

$$\varphi(\mathbf{r}) = \varphi_{\text{ext}}(\mathbf{r}) + \sum_{lm} \frac{s_l}{s(\omega) - s_l} \mathrm{I}_{lm} \psi_{lm}(\mathbf{r}) \tag{40}$$

Using,

$$\frac{s_l}{s(\omega) - s_l} = -\frac{\varepsilon_\mathrm{m}(\omega) - \varepsilon_\mathrm{d}}{\left[\varepsilon_\mathrm{m}(\omega) + \{\varepsilon_\mathrm{d}(l+1)/l\} \right]} \tag{41}$$

we finally get,

$$\varphi(\mathbf{r}) = \varphi_{\text{ext}}(\mathbf{r}) + \frac{4\pi \mathrm{p}_\mathrm{j}}{\varepsilon_\mathrm{d}} \sum_{lm} \frac{\varepsilon_m(\omega) - \varepsilon_d}{\left[\varepsilon_\mathrm{m}(\omega) + \{\varepsilon_\mathrm{d}(l+1)/l\} \right]} \frac{(l+1)}{(2l+1)} \frac{1}{\mathrm{R}\,\mathrm{r}_\mathrm{j}} \left(\frac{\mathrm{R}^2}{\mathrm{r}\,\mathrm{r}_\mathrm{j}} \right)^{l+1} \mathrm{Y}^*_{l\mathrm{m}}(\theta_j, \phi_j) \mathrm{Y}_{l\mathrm{m}}(\theta, \varphi) \tag{42}$$

When both molecules are placed on the z-axis and their orientation is also parallel to the +z-axis, $\mathrm{Y}_{l\mathrm{m}}(0,0) = \mathrm{Y}^*_{l0}(0,0) = \sqrt{(2l+1)/4\pi}$. We can therefore write,

$$\varphi(\mathbf{r}) = \varphi_{ext}(\mathbf{r}) + \frac{p_j}{\varepsilon_d}\sum_{lm}\frac{\varepsilon_m(\omega)-\varepsilon_d}{[\varepsilon_m(\omega)+\{\varepsilon_d(l+1)/l\}]}\frac{(l+1)}{R\,r_j}\left(\frac{R^2}{r\,r_j}\right)^{l+1} \tag{43}$$

The radial component of the electric field can be written as,

$$\mathbf{E}(\mathbf{r}) = -\nabla\varphi(\mathbf{r}) = \mathbf{E}_{ext}(\mathbf{r}) + \frac{p_j}{\varepsilon_d R^3}\sum_{l}\frac{(l+1)^2[\varepsilon_m(\omega)-\varepsilon_d]}{[\varepsilon_m(\omega)+\{\varepsilon_d(l+1)/l\}]}\left(\frac{R^2}{r\,r_j}\right)^{l+2} \tag{44}$$

If $\mathbf{r}$ is chosen to be the location of the acceptor molecule (the field there is denoted below as $\mathbf{E}_a$) and j[th] molecule is taken to be a donor, the plexcitonic coupling (or, SP dressed dipolar interaction energy) $J(\omega)$ can be written as,

$$J(\omega) = -\mathbf{p_a}\bullet\mathbf{E}_a = \frac{-2\,p_a p_d}{\varepsilon_d|r_d-r_a|^3} - \frac{p_a p_d}{\varepsilon_d R^3}\sum_{l}\frac{(l+1)^2[\varepsilon_m(\omega)-\varepsilon_d]}{[\varepsilon_m(\omega)+\{\varepsilon_d(l+1)/l\}]}\left(\frac{R^2}{r_a r_d}\right)^{l+2} \tag{45}$$

We have also presented an alternative derivation of Eq. 45 in the Appendix, based on the direct method. We can now define the interaction energy enhancement factor $A(\omega)$ similar to Ref. 14 as,

$$A^{NSP}(\omega) = 1 + \frac{1}{2}\left(\frac{|r_d-r_a|}{R}\right)^3\sum_{l}\frac{(l+1)^2[\varepsilon_m(\omega)-\varepsilon_d]}{[\varepsilon_m(\omega)+\{\varepsilon_d(l+1)/l\}]}\left(\frac{R^2}{r_a r_d}\right)^{l+2} \tag{46}$$

It should be mentioned that Eq. 46 differs from Eq. 11 of Ref. 14 due to the fact that the molecules there were considered to be on the diametrically opposite sides of the particle. The present case corresponds to the molecules located on the same side, the situation relevant to the molecular nanojunction. Using Eq. 45, the characteristic frequency (ω_l) of the l-th mode (where, $l = 1, 2, 3....$ etc. signifies dipolar, quadrupolar and other higher order modes, respectively) can be described as,

$$\varepsilon_m(\omega) = -\frac{(l+1)}{l}\varepsilon_d \tag{47}$$

Eq. 47 defines the resonance condition corresponding to l-th mode and is the same as obtained in [23]. The approach was further extended to the nanoshell (NSH) geometry (see, Fig. 1.b), whose details will be presented in the subsequent publications. The amplification factor for NSH is obtained as,

$$A^{NSH}(\omega) = 1 + \frac{1}{2}\left(\frac{|r_d-r_a|}{b}\right)^3\sum_{l}(l+1)^2\left(\frac{R^2}{r_a r_d}\right)^{l+2}\left[\begin{array}{c}\dfrac{[\varepsilon_m(\omega)-\varepsilon_d]}{\left\{\dfrac{4\lambda_l(l+1)}{(\lambda_l+1)(2l+1+\lambda_l)}\right\}\left\{\varepsilon_m(\omega)+\varepsilon_d\dfrac{(2l+1+\lambda_l)}{(2l+1-\lambda_l)}\right\}} \\ + \\ \dfrac{[\varepsilon_m(\omega)-\varepsilon_d]}{\left\{\dfrac{4\lambda_l(l+1)}{(\lambda_l-1)(2l+1-\lambda_l)}\right\}\left\{\varepsilon_m(\omega)+\varepsilon_d\dfrac{(2l+1-\lambda_l)}{(2l+1+\lambda_l)}\right\}}\end{array}\right] \tag{48}$$

where, $\lambda_l = \sqrt{1+4l(l+1)x^{2l+1}}$, and x denotes the inner to outer radius of NSH, which is also referred to as the NSH aspect ratio [10]. As expected, Eq. 48 for NSH monomer converges to the corresponding NSP expression in the limiting case, x=0. In contrast to the single resonant

frequency in NSP, NSH spectra exhibit two characteristic frequencies for each polarity index. This is due to the interaction between sphere and cavity plasmons, which induces surface charges at the inner and the outer interface of NSH. In the passing, we would like to mention that for the incident (exciting) field parallel to the axis, the m=0 mode (longitudinal polarization of the field) is the only active mode and also known to give the most significant shifts [24]. Also, when field is perpendicular to the chain axis (transversal polarization), only the degenerate mode $m = \pm 1$ will be active [23]. To extend MSE based approach to the NSP dimer, an interaction matrix approach based on using the eigenstates of the single inclusion [17, 18] has been used.

3. Results and Discussions

In this section, we present the results of our study of a monomer of a nanosphere and nanoshell as well as the dimer of nanosphere. The metal considered to be silver is modeled using Drude-Lorentz model based frequency dependent dielectric function and is defined as,

$$\varepsilon_m(\omega) = \varepsilon_0 - \frac{\omega_p^2}{\omega(\omega + \mathbf{i}\gamma)} \tag{49}$$

where, ω is the excitation frequency, ω_p is the bulk plasma frequency, and γ is the damping constant due to scattering of metal electrons. The values of Drude parameters, ε_0, ω_p and γ used for present analysis are, 3.57, 9.1 eV, and 0.052 eV, respectively. Unless mentioned otherwise, the dielectric constant of the embedded medium $\varepsilon_d = 2.0$, equal dipole moments $\mathbf{p}_a$ and $\mathbf{p}_d$=10 D (Debye), the distance between the nearest molecule and the metal surface equal to 1.0 nm, and intermolecular distance of 1.0 nm will be used. For brevity a three index notation (u,v,w) will be used where first index (u) will refer to the radius (of NSP) or outer radius (of NSH), second index (v) will refer to the distance of the closest molecule from the surface, and the third index (w) will refer to the intermolecular separation in nanometers. Figure 2 shows the spectral variation of |J| [Fig. 2.a], A (ω) [Fig. 2.b], Re {J} [Fig. 2.c], and Im{J} [Fig. 2.d] for NSP monomer of different sizes (R=10, 20, 30, 40 &50 nm). The main features of Fig. 2 can be summarized as: (I). Appearance of sharp resonant peak at ~ ω =3.82 eV in the J spectrum for all sizes. This resonant position corresponds to the high order multipolar resonance limit as can be seen from the analytical condition, $\varepsilon_m(\omega) = -\varepsilon_d\left[(l+1)/l\right]$, (II). Slight blue-shift of the resonant position with increasing the J value, and disappearance of lower frequency peaks with the increase in NSP size. These features are due to the fact that sphere with greater size will support higher order surface plasmon modes which are dominant. For smaller sizes, as expected, lower orders (e.g., dipolar, quadrupolar etc.) become stronger and peaks originated from lower order multipoles can also become visible, (III). For NSP sizes well-suited to the quasitatic limitations, enhancement factor A (ω) > 2 is achievable when molecular transition frequency coincides with the dominant plasmon frequency of NSP. We would like to emphasize that the large enhancement of A (ω) reported in [14] and of a similar quantity (FRET rate γ_F) in [10] corresponds to the negligibly small bare interaction by virtue of the large molecular separation. In the present system under consideration where bare interaction (~ 0.06 eV) itself is strong, the enhancement factor > 2 is significant and may lead to important changes in molecular nanojunction characteristics. By virtue of the presence of the metal, J will bear now complex characteristics i.e., real and imaginary parts, which are separately shown in Figs. 2.c and 2.d, respectively.

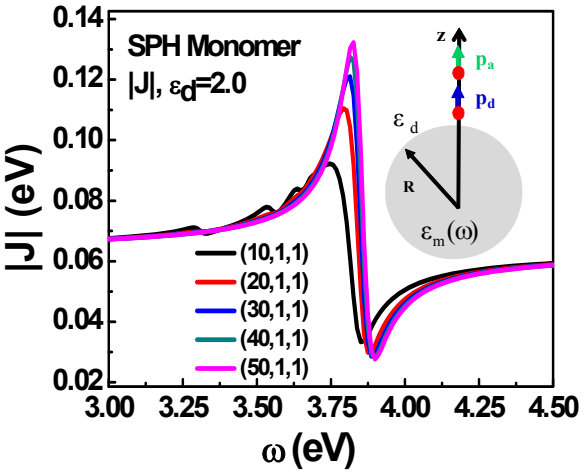

Fig. 2(a): The calculated variation of |J| as a function of the molecular transition frequency (ω) in the proximity of NSP monomer with variable size (R=10, 20, 30, 40 & 50 nm). Evidently, strong resonant feature ~ 3.82 eV (U.V) appears for all sizes. Moreover, relatively higher enhancement with increased size is observed. Other parameters are: ε_d =2.0, $\mathbf{p}_a$ and $\mathbf{p}_d$=10 D.

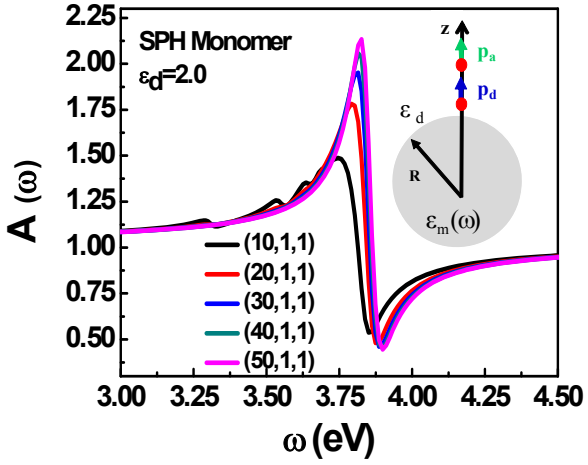

Fig. 2(b): The calculated variation of enhancement factor A(ω) [Eq. 46] as a function of the molecular transition frequency (ω) in the proximity of NSP monomer with variable size (R=10, 20, 30, 40 & 50 nm). Evidently > 2 fold enhancement near dominant plasmon frequency is obtained. Other parameters are: ε_d =2.0, $\mathbf{p}_a$ and $\mathbf{p}_d$=10 D.

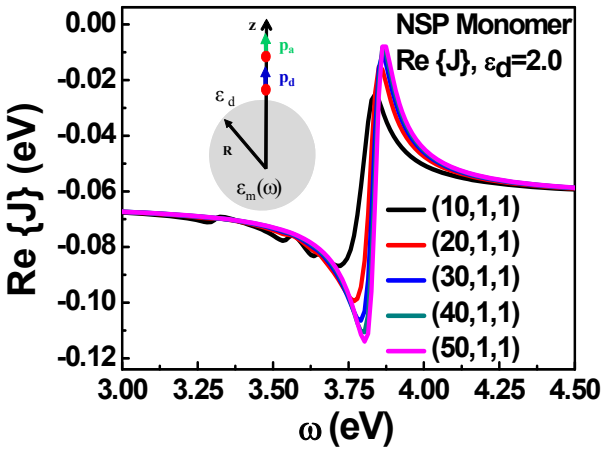

Fig. 2(c): The calculated variation of Re{J} as a function of the molecular transition frequency (ω). Other parameters are similar to those of Fig. 2(a).

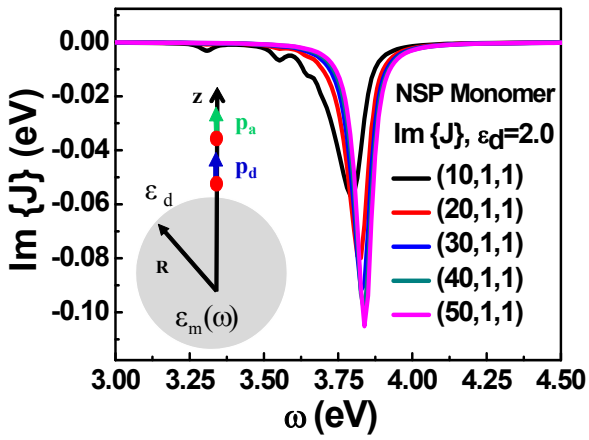

Fig. 2(d): The calculated variation of Im{J} as a function of the molecular transition frequency (ω). Other parameters are similar to those of Fig. 2(a).

Next, aiming to understand the effect of host medium, we present spectral variation of |J| [Fig. 3.a], and A (ω) [Fig. 3.b] for NSP monomer specified as (50,1,1) and considered embedded into different host mediums [ε_d=1.0 (vacuum), 1.5. 2.0, 2.5, and 3.0]. The central features of Fig. 3 can be summarized as: (I). Reduction in J, and red-shift of the resonant peak position with increased dielectric constant ε_d of the of the host medium, also analytically understandable using resonance condition, $\mathrm{Re}[\varepsilon_m(\omega)] = -\varepsilon_d\left[(l+1)/l\right]$. The use of Drude model gives, $\mathrm{Re}[\varepsilon_m(\omega)] = \varepsilon_0 - (\omega_p^2/\omega_{Res}^2)$, where ω_{Res} denotes the resonant frequency, which for an arbitrary multipole l can be written as, $\omega_{Res} = \omega_p/\sqrt{\left[\varepsilon_0 + \{\varepsilon_0\,(l+1)/l\}\right]}$. (III). Increased enhancement factor A (ω) with increasing ε_d (see, Fig. 3.b). This attribute may be important for sensing applications, (III). For NSP sizes well-suited to the quasitatic limitations, enhancement factor A (ω) > 2 is achievable when the molecular transition frequency coincides with the dominant plasmon frequency of NSP.

In addition to the enhancement of the molecular interaction J, the energy transfer from the molecules to the metallic nanostructure is an important process as it competes with the molecular energy transfer. The results of our estimation are shown in Fig. 4, where we have also shown the spectral variation of |J| and γ_m (γ_m estimation is based on Ref. 10), and the comparison of Re{J} and Im{J} for NSP (50,1,1). It can be noticed that the peak positions of |J| and γ_m are shifted relative to each other. Through an appropriate choice of molecular transition frequency, enhancement can be maximized while γ_m still remains relatively small.

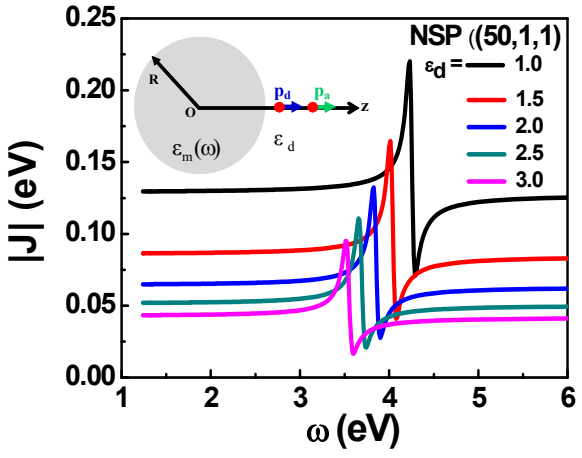

Fig. 3(a): The calculated variation of |J| as a function of the molecular transition frequency (ω), in the proximity of NSP monomer of R=50 nm and variable host mediums (ε_d=1.0, 1.5, 2.0, 2.5, and 3.0).

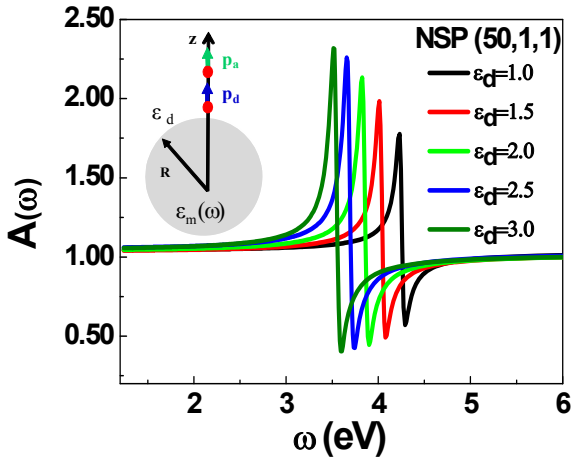

Fig. 3(b): The calculated variation of A(ω), the enhancement factor, as a function of the molecular transition frequency (ω). Other parameters are similar to those of Fig. 3(a). Evidently, A (ω) > 2 can be achieved for practical ε_d.

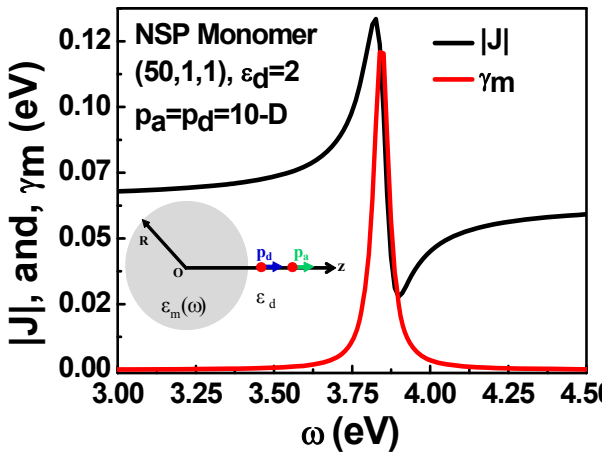

Fig. 4(a): The calculated variation of |J| and the loss to the metal γ_m as a function of the molecular transition frequency (ω) in the proximity of NSP monomer of R=50 nm in the medium characterized by dielectric constant ε_d=2.0.

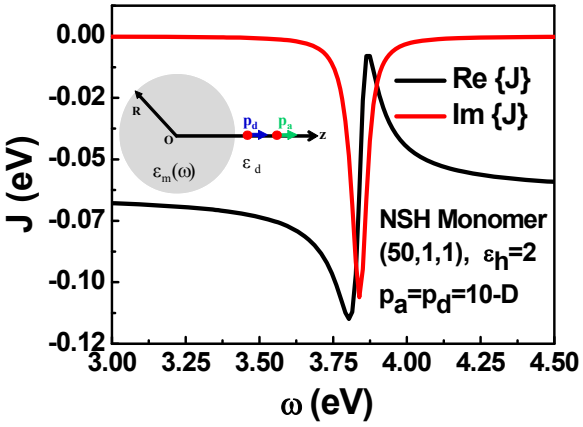

Fig. 4(b): The calculated variation of real and imaginary parts of J as a function of the molecular transition frequency (ω) in the proximity of NSP monomer of R=50 nm in the medium characterized by dielectric constant ε_d=2.0.

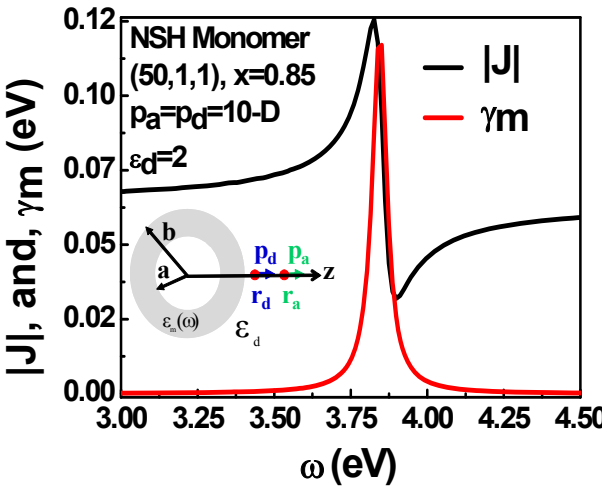

Fig. 5(a): The calculated variation of |J| and the loss (γ_m) to the metal as a function of the molecular transition frequency (ω) in the proximity of NSH monomer of outer radius 50 nm and aspect ratio=0.85 in the medium characterized by dielectric constant ε_d=2.0.

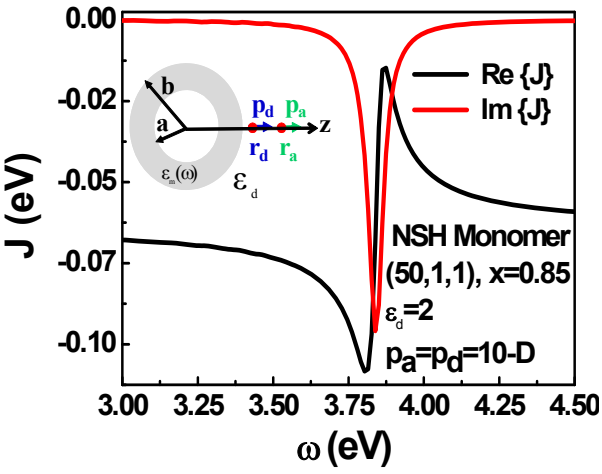

Fig. 5(b): The calculated variation of real and imaginary part of J as a function of the molecular transition frequency (ω) in the proximity of NSH monomer of outer radius 50 nm and aspect ratio=0.85 in the medium characterized by dielectric constant ε_d=2.0.

Next, we consider a monomer nanoshell (NSH), keeping other parameters similar to those of the NSP geometry. Figure 5 shows the variation of $|J|, \gamma_m$, Re{J} and Im{J} for monomer NSH (50,1,1) with aspect ratio 0.85. It can be seen that the variation is similar to that of the sphere. Similar to NSP, NSH also enhances the interaction.

Finally, we consider a dimer of two identical silver NSPs of radius R=10 nm, surface to surface gap=3 nm, surface-molecule separation=1.0 nm, molecular separation=1.0 nm. The results of our calculation of |J| are shown in Fig. 6. In order to compare, corresponding NSP monomer data (right sphere is removed) is also shown. The main features can be summarized as: (I). In contrast to the monomer NSP, the spectrum of |J| now shows multiple peaks, where maximum enhancement can be achieved, this is due to the hybridization of the plasmons belonging to individual NSPs [7], (II). While monomer shows a single dominant resonance, dimer shows multiple resonances, red-shifted relative to the monomer, (III). An enhancement greater than that of a monomer NSP can be obtained in a wide spectral window, (IV). Since dimer geometry imitates a real molecular junction, an overall enhancement in the junction characteristics can be expected.

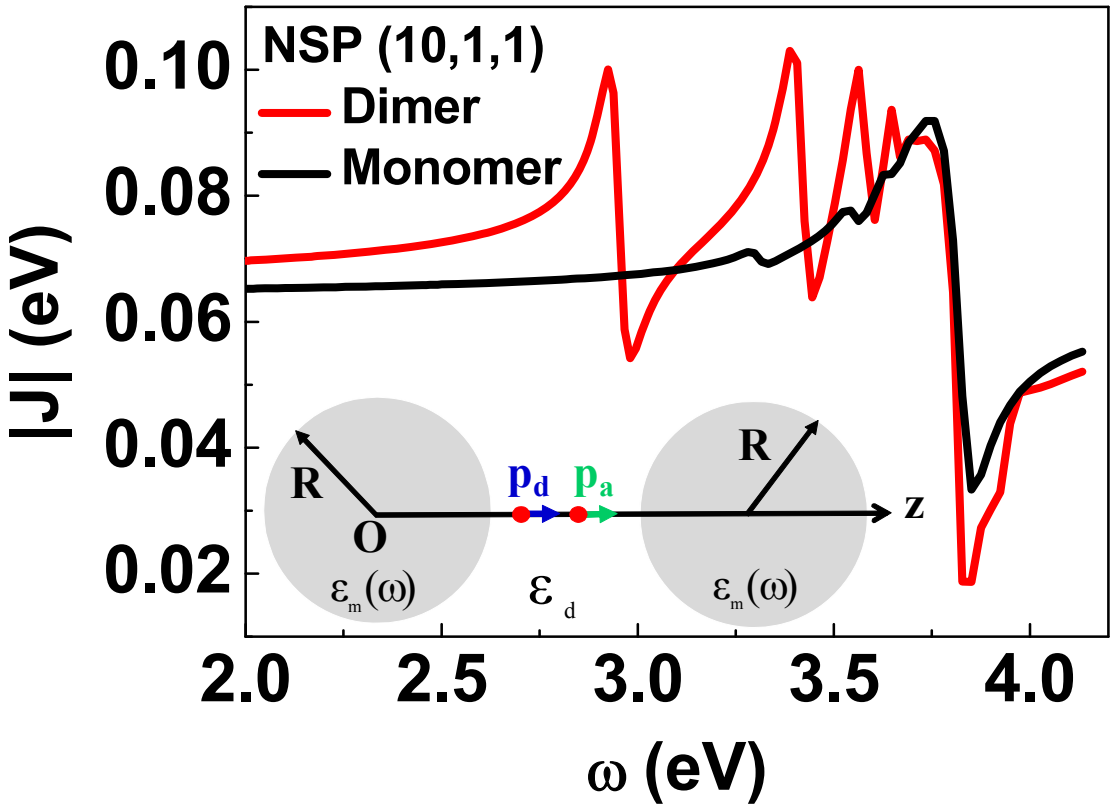

Fig. 6: The calculated variation of the absolute value of J as a function of the molecular transition frequency (ω) for the molecular pair placed in the dimer junction region. Radii of each NSP are 10 nm, intermolecular distance is 1 nm and the distance of each molecule from the closest NSP is 1-nm. The dielectric constant of the embedding medium is ε_d=2.0. Also the data for the monomer (when only the left NSP is present) are shown.

4. Conclusions

We have developed a theoretical model for evaluating energy transfer interactions in the proximity of metallic nanostructures such as nanosphere and nanoshell particles and their coupled dimer. The enhancement factor > 2 is predicted for practical geometries. NSP dimer shows rich spectral features and greater enhancement relative to the monomer. The role of size and dielectric environment on energy transfer interaction is investigated. The influence of the enhancement of energy transfer interaction on current in molecular nanojunction [13] will be studied elsewhere.

Acknowledgements

Authors acknowledge Professor D. J. Bergmann (Tel Aviv University) for valuable discussions. MSS gratefully acknowledge his colleague Michal Oren (Tel Aviv University) for her vital help in understanding the spectral method. This work was supported by the German-Israeli Fund (A.N.), European Research Commission and the Israel Science Foundation (A.N.), the Israel-U.S. Binational Science Foundation (A.N. and B.F.), and the Russia-Israel Scientific Research Cooperation (B.F.).

Appendix

This appendix briefly presents the main steps for solving the problem considered in Sec. 2 using direct approach. The electrostatic potential inside and outside NSP monomer can be written as,

$$\Phi(\mathrm{r}) = \begin{cases} \sum_{lm} \mathrm{P}_{lm}\, \mathrm{r}^{l} \mathrm{Y}_{l\mathrm{m}}(\theta,\phi) & \text{for } \mathrm{r} < \mathrm{R} \\ \sum_{lm} \mathrm{Q}_{lm} \dfrac{1}{\mathrm{r}^{l+1}} \mathrm{Y}_{l\mathrm{m}}(\theta,\phi) + \Phi_d + \Phi_a & \text{for } \mathrm{r} > \mathrm{R} \end{cases} \tag{A.1}$$

where, $\Phi_d\,(\Phi_a)$ denotes dipolar potential associated with donor (acceptor) molecule, and may be written as, (for definiteness consider $r > r_{d(a)}$, although it will not affect the final result).

$$\Phi_{d(a)}(\mathrm{r}) = \frac{4\pi \mathrm{p}_{d(a)}}{\varepsilon_{\mathrm{d}}} \sum_{lm} \frac{l}{(2l+1)} \left(\frac{\mathrm{r}_{d(a)}^{l-1}}{\mathrm{r}^{l+1}} \right) \mathrm{Y}^{*}_{l'\mathrm{m}}(\theta_{d(a)}, \phi_{d(a)}) \mathrm{Y}_{l,\mathrm{m}}(\theta,\phi) \tag{A.2}$$

where symbols have their standard physical definitions. The radial derivative can be written as,

$$\Phi'_{d(a)}(\mathbf{r}) = -\frac{4\pi \mathrm{p}_{d(a)}}{\varepsilon_{\mathrm{d}}} \sum_{lm} \frac{l(l+1)}{(2l+1)} \left(\frac{\mathrm{r}_{d(a)}^{l-1}}{\mathrm{r}^{l+2}} \right) \mathrm{Y}^{*}_{l\mathrm{m}}(\theta_{d(a)}, \phi_{d(a)}) \mathrm{Y}_{lm}(\theta,\phi) \tag{A.3}$$

Imposing electrostatic boundary conditions (continuity of Φ and $\mathbf{D}_{\perp}$ at NSP surface) and assuming that we want to calculate the potential at the location of the acceptor (in this case the effect of the acceptor will be removed) produces,

$$\mathrm{P}_{lm} = -\frac{4\pi \mathrm{p}_d}{\varepsilon_{\mathrm{d}}\, \mathrm{r}_d^{l+2}} \frac{\mathrm{Y}^{*}_{l\mathrm{m}}(\theta_d, \phi_d)}{\left\{ 1 + \dfrac{\varepsilon_{\mathrm{m}}(\omega)}{\varepsilon_{\mathrm{d}}} \dfrac{l}{(l+1)} \right\}} \tag{A.4}$$

$$Q_{lm} = \frac{4\pi p_d}{\varepsilon_d}\frac{R^{2l+1}}{r_d^{l+2}}\left[\frac{(l+1)}{(2l+1)} - \frac{1}{\left\{1+\frac{\varepsilon_m(\omega)}{\varepsilon_d}\frac{l}{(l+1)}\right\}}\right]Y^*_{l'm}(\theta_d,\phi_d) \quad (A.5)$$

The induced potential at the acceptor site can be written as,

$$\Phi^{out}_{ind}(\mathbf{r}=\mathbf{r}_a) = \sum_{lm}\frac{4\pi p_d}{\varepsilon_d}\frac{R^{2l+1}}{r_a^{l+1}r_d^{l+2}}\left[\frac{(l+1)}{(2l+1)} - \frac{1}{\left\{1+\frac{\varepsilon_m(\omega)}{\varepsilon_d}\frac{l}{(l+1)}\right\}}\right]Y^*_{lm}(\theta_d,\phi_d)Y_{lm}(\theta_a,\phi_a) \quad (A.6)$$

The induced electric field at the acceptor site is,

$$\mathbf{E}^{out}_{ind}(\mathbf{r}=\mathbf{r}_a) = \sum_{lm}\frac{4\pi p_d}{\varepsilon_d}\frac{R^{2l+1}}{r_a^{l+2}r_d^{l+2}}\frac{(l+1)^2}{(2l+1)}\frac{[\varepsilon_m(\omega)-\varepsilon_d]}{\left[\varepsilon_m(\omega)+\{\varepsilon_d(l+1)/l\}\right]}Y^*_{l'm}(\theta_d,\phi_d)\,Y_{l'm}(\theta_a,\phi_a) \quad (A.7)$$

The induced plexcitonic coupling (or SP dressed dipolar interaction energy) $J_{ind}(\omega)$ can be written as,

$$J_{ind}(\omega) = -\sum_{lm}\frac{4\pi p_a p_d}{\varepsilon_d}\frac{R^{2l+1}}{r_a^{l+2}r_d^{l+2}}\frac{(l+1)^2}{(2l+1)}\frac{[\varepsilon_m(\omega)-\varepsilon_d]}{\left[\varepsilon_m(\omega)+\{\varepsilon_d(l+1)/l\}\right]}Y^*_{l'm}(\theta_d,\phi_d)\,Y_{l'm}(\theta_a,\phi_a)$$

For the location of molecules on the symmetry axis,

$$J_{ind}(\omega) = -\frac{p_a p_d}{\varepsilon_d R^3}\sum_l\frac{(l+1)^2[\varepsilon_m(\omega)-\varepsilon_d]}{\left[\varepsilon_m(\omega)+\{\varepsilon_d(l+1)/l\}\right]}\left(\frac{R^2}{r_a\,r_d}\right)^{l+2} \quad (A.8)$$

The total dipolar interaction energy can be written as,

$$J(\omega) = \frac{-2p_a p_d}{\varepsilon_d|r_d-r_a|^3} - \frac{p_a p_d}{\varepsilon_d R^3}\sum_l\frac{(l+1)^2[\varepsilon_m(\omega)-\varepsilon_d]}{\left[\varepsilon_m(\omega)+\{\varepsilon_d(l+1)/l\}\right]}\left(\frac{R^2}{r_a r_d}\right)^{l+2} \quad (A.9)$$

Eq. (A.9) coincides with Eq. 45.

References

[1]. Stefan Maier, "Plasmonics fundamentals and applications", Springer (2007).

[2]. K. L. Kelly, E. Coronado, L. L. Zhao, and G. C. Schatz, "The optical properties of metal nanoparticles: The influence of size, shape, and dielectric environment", J. Phys. Chem. B **107**, 668 (2003).

[3]. J. B. Lassiter, J. Aizpurua, L. I. Hernandez, D. W. Brandl, I. Romero, S. Lal, J. H. Hafner, P. Nordlander, and Naomi J. Halas, "Close encounters between two nanoshells", Nano Lett., **8**, 1212 (2008).

[4]. J. W. Liaw, "Local-Field Enhancement and Quantum Yield of Metallic Dimer", Japanese Journal of Applied Physics, **46,** 5373 (2007).

[5]. K. Li, M. I. Stockman, and D. J. Bergman, "Self-similar chain of metal nanospheres as an efficient nanolens", Physical Review Letters, **91**, 227402 (2003).

[6]. V. A Markel, "Coherently tunable third-order nonlinearity in a nanojunction", J. Phys. B: At. Mol. Opt. Phys. **38**, L347–L355 (2005).

[7]. E. Prodan, C. Radloff, N. J. Halas, and P. Nordlander, "A hybridization model for the plasmon response of complex nanostructures", Science **302**, 419 (2003).
[8]. P. Nordlander and C. Oubre, "Plasmon hybridization in nanoparticle dimers", Nano Lett. **4**, 899 (2004).
[9]. S. J. Oldenburg, G. D. Hale, J. B. Jackson, and N. J. Halasa, "Light scattering from dipole and quadrupole nanoshell antennas", Appl. Phys. Lett **75,** 1063 (1999).
[10]. M. Durach, A. Rusina, V. I. Klimov, and M. I. Stockman, "Nano-plasmonic renormalization and enhancement of Coulomb interactions", New Journal of Physics **10**, 105011 (2008).
[11]. O. Govorov, J. Lee, and N. A. Kotov, "Theory of plasmonic enhanced Forster energy transfer in optically excited semiconductor and metal nanoparticles", Phys. Rev. B **76**, 125308 (2007).
[12]. X. R. Su, W. Zhang, L. Zhou, X. N. Peng, Q. Q. Wang, "Plasmon enhanced Forster energy transfer between semiconductor quantum dots: multipole effects", Optics Exp. **18**, 6516 (2010).
[13]. G. Li, B.D. Fainberg, A. Nitzan, S. Kohler and P. Hanggi, "Coherent charge transport through molecular wires: Exciton blocking and current from electronic excitations in the wire", Phys. Rev. B, **81**,165310 (2010).
[14]. J. I. Gersten, A. Nitzan, "Accelerated energy transfer between molecules near a solid particle", Chem. Phys. Lett. **104**, 31(1984).
[15]. X. M. Hua, J. I. Gersten, and A. Nitzan, "Theory of energy transfer between molecules near solid state particles", J. Chem. Phys. **83**, 3650 (1985).
[16]. R. Fuchs, "Theory of the optical properties of ionic crystal cubes", Phys. Rev. B **11**, 1732 (1975).
[17]. D. J. Bergman, Phys. Rep. **43**, 377 (1978).
[18]. D. J. Bergman, "Dielectric constant of a two-component granular composite: A practical scheme for calculating the pole spectrum", Phys. Rev. B, **19**, 2359 (1979).
[19]. G. W. Milton, "Bounds on the complex dielectric constant of a composite mater", Appl. Phys. Lett. **37**, 300 (1980)
[20]. M. I. Stockman, S. V. Faleev, and D. J. Bergman, "Localization versus delocalization of surface plasmons in nanosystems: Can one state have both characteristics?", Phys. Rev. Lett. **87**, 167401 (2001).
[21]. J. D. Jackson, "Classical Electrodynamics", John Wiley & Sons, (1998).
[22]. D. J. Griffiths, "Introduction to electrodynamics", Prentice Hall, ISBN 013-80-5326-X (1999).
[23]. J. M. Gerardy and M. Ausloos, "Absorption spectrum of clusters of spheres from the general solution of Maxwell's equations: The long-wavelength limit", Phys. Rev. B, **22**, 4950 (1980).
[24]. E. R. Encina, and E. A. Coronado, "Plasmon coupling in silver nanosphere pairs", J. Phys. Chem. C, **114**, 3918 (2010).